LA-UR-04-2449, Strain Journal, 40(2), 49-58, 2004

Estimation of Electric Charge output for Piezoelectric Energy Harvesting

Henry A. Sodano and Daniel J. Inman
Center for Intelligent Material Systems and Structures
Virginia Polytechnic Institute and State University
Blacksburg, VA 24061

Gyuhae Park
Engineering Sciences and Applications
Weapon Response Group
Los Alamos National Laboratory
Los Alamos, NM 87545

Abstract

Piezoelectric materials can be used as mechanisms to transfer mechanical energy, usually ambient vibration, into electrical energy that can be stored and used to power other devices. With the recent advances in wireless and MEMS technology, sensors can be placed in exotic and remote locations. Since these devices are wireless it becomes necessary that they have their own power supply. The power supply in most cases is the conventional battery; however, problems can occur when using batteries because of their finite life span. Because most sensors are being developed so that they can be placed in remote locations such as structural sensors on a bridge or GPS tracking devices on animals in the wild, obtaining the sensor simply to replace the battery can become a very expensive task. Furthermore, in the case of sensors located on civil structures it is often advantageous to embed them, making access impossible. Therefore, if a method of obtaining the untapped energy surrounding these sensors was implemented, significant life could be added to the power supply. One method is to use piezoelectric materials to obtain ambient energy surrounding the test specimen. This captured energy could then be used to prolong the life of the power supply or in the ideal case provide endless energy for the sensors lifespan. The goal of this study is to develop a model of the piezoelectric power harvesting device. This model would simplify the design procedure necessary for determining the appropriate size and vibration levels necessary for sufficient energy to be produced and supplied to the electronic devices. An experimental verification of the model is also performed to ensure its accuracy.

Nomenclature

α = proportional damping constant

a = acceleration

A = amplitude of vibration

β = proportional damping constant

b = width of beam

c = modulus of elasticity

C_p = capacitance of piezoelectric

C = damping matrix

δ = variation

d_{ij} = piezoelectric constant relating voltage and stress

D = Electric Displacement

E = electric field

e = piezoelectric coupling coefficient

f = external force

K = stiffness

L = length of beam

M = mass

φ = location of electrical potential

q = electrical charge

ρ = density

r = temporal coordinate of displacement

R = resistance

ε = dielectric constant

S = strain

t = thickness of beam or time

t_p = thickness of piezoelectric

T = kinetic energy or stress in piezoelectric constitutive equations

θ = piezoelectric coupling matrix

u = displacement

U = potential energy

v = voltage

V = volume

V.I. = variational indicator

Φ = mode shapes

ω = natural frequency

ζ = damping ratio

Superscript

E = parameter at constant electrical field (short circuit)

S = Value taken at constant strain

T = parameter at constant stress or transpose

Subscript

p = piezoelectric

s = structure

Introduction

The idea of building portable electronic devices or wireless sensors that do not rely on power supplies with a limited lifespan has intrigued researchers and instigated a sharp increase in research in the area of power harvesting. One method of power harvesting is to use piezoelectric materials, which form transducers that are able to interchange electrical energy and mechanical strain or force. Therefore, these materials can be used as mechanisms to transfer ambient motion (usually vibration) into electrical energy that may be stored and used to power other devices. By implementing power harvesting devices, portable systems can be developed that do not depend on traditional methods for providing power, such as the battery, which has a limited operating life.

A significant amount of research has been devoted to developing and understanding power harvesting systems. These studies, demonstrate the feasibility of using piezoelectric devices as power sources. One early studied performed by Umeda et al (1996) investigated the power generated when a free-falling steel ball impacted a plate with a piezoceramic wafer attached to its underside. Their study used an electrical equivalence model to simulate the energy generated and calculate the efficiency of the PZT's ability to transform mechanical impact energy

into electrical power. It was found that a significant amount of the impact energy was returned to the ball in the form of kinetic energy during the balls rebound off of the pate, however, it is stated that if the ball stuck to the plate an efficiency of 52% could be achieved. In a later paper, Umeda et al (1997) investigated the energy storage characteristics of a power harvesting system consisting of a PZT, full-bridge rectifier and a capacitor. Their work discussed the effect of various parameters on the efficiency of the storage circuit. Following their analytic investigation a prototype was developed and stated to have an efficiency of over 35%, more than three times greater than a solar cell. Starner (1996) examines the possible location for power harvesting devices around the human body and surveys the energy available from sources of mechanical energy including blood pressure, walking, and upper limb motion of a human being. The author claims 8.4 watts of useable power can be achieved from a PZT mounted in a shoe. Kymissis et al (1998) examines using a piezofilm in addition to a Thunder actuator (http://www.face-int.com), to charge a capacitor and power a RFID transmitter from the energy lost to the shoe during walking. The polyvinylidene fluoride (PVDF) stave was located in the sole to absorb the bending energy of the shoe, and the piezoceramic thunder actuator was located in the heel to harvest the impact energy. Their work showed that the power generated by the piezoelectric devices was sufficient for powering functional wireless devices and were able to transmit a 12-bit signal five to six times every few seconds. Following the work of Kymssis et al (1998), the research involving wireless sensors began to grow, and in 1998, Kimura received a US Patent that centered on the use of a vibrating piezoelectric plate to generate energy sufficient to run a small transmitter fixed to migratory birds for the purpose of transmitting their identification code and location. The effectiveness of the power harvesting system is also compared to existing battery technology. Goldfarb et al (1999) presented a linearized model of a PZT stack and analyzed its efficiency as a power generation device. It was shown that the maximum efficiency occurs in a low frequency region, much lower than the structural resonance of the stack. It is also stated that the efficiency is also related to the amplitude of the input force due to hysteresis of the PZT. In addition to the force applied in the poling direction (d_{33} mode), Clark and Ramsay (2000) have investigated and compared it with the transverse force (d_{31} mode) for a PZT generator. There work showed that the d_{31} mode has a mechanical advantage in converting applied pressure to working stress for power generation. They concluded that a 1-cm^2 piezoceramic wafer can power a MEMS device in the microwatt range. Elvin et al (2001) theoretically and experimentally investigated a self-powered wireless sensors using PVDF. The power harvesting system used the energy generated by the PVDF to charge a capacitor and power a transmitter that could send information regarding the strain of the beam a distance of 2m. Kasyap et al (2002) formulated a lumped element model

to represent the dynamic behavior of PZT in multiple energy domains using an equivalent circuit. Their model has been experimentally verified using a 1-d beam structure with peak power efficiencies of approximately 20%.

Most of the previous studies all realized that the energy generated by the piezoelectric material must be accumulated before it can be used to power other electronic devices. Rather than use the traditional capacitor that most other studies used, Sodano et al (2002) investigated the use of rechargeable batteries to accumulate the generated energy. The goal of this study was to show that the small amounts of ambient vibration found on a typical system could be used to charge the battery from its discharged state and demonstrated the compatibility of rechargeable batteries and the power generated by piezoelectric materials. To do this, the vibration of the air compressor of a typical automobile was measured and a similar signal was applied to an aluminum plate with a piezoelectric patch attached. It was found that the random signal from the engine compartment of a car could charge the battery in only a couple of hours and that a resonant signal could charge the battery in under an hour. Ottman et al (2002) realized that if circuitry was used to maximize the energy generated then these storage devices could be charged with greater efficiency. Therefore, they investigated the effects of utilizing a DC-DC step down converter with an adaptive control algorithm to maximize power output of the piezoelectric material. Their efforts found that when using the adaptive circuit, energy was harvested at over four times the rate of direct charging without a converter.

The work that will be presented in this document concentrates on developing an analytic model of a beam with piezoelectric elements attached that will provide an accurate estimate of the power generated through the piezoelectric effect. It has been found in previous studies that piezoelectric material attached to a beam with cantilever boundary conditions provides an effective configuration for capturing transverse vibrations and converting them into useful electrical power. This configuration has proven itself to be effective in several experiments carried out by Sodano et al 2002 and Sodano et al 2003. The model detailed in this paper is based off of a more general one developed by Hagood et al. (1990) to estimate the performance of piezoelectric shunt damping circuits for passive vibration control. In addition, the model developed in Crawley et al. (1990) was used to develop the actuation equations for piezoelectric devices and the constitutive equations of bimorph actuators were obtained from Smits et al. (1991). However, an important addition is made to the combination of these models to accommodate power harvesting, which was neglected in previous models, was to add material

damping; if excluded the model can predict significantly more energy generation that actually developed in the real system. The following sections will develop a model of the piezoelectric power harvesting device. This model would simplify the design procedure necessary for determining the appropriate size and extent of vibration needed for sufficient energy to be produced and supplied to the desired electronic devices. An experimental verification, of the model is also performed to ensure its accuracy. Following the verification of the model, the effects of power harvesting on the dynamics of a structure are compared to those brought on from shunt damping.

Model of Piezoelectric Power Harvesting Beam

The following derivation will use energy methods to develop the constitutive equations of a bimorph piezoelectric cantilever beam for power harvesting. To begin the deviation we will start with the general form of Hamilton's Principle. This states that the variational indicator must be zero at all time, as shown below in equation 1:

$$\text{V.I.} = \int_{t_1}^{t_2} \left[\delta T - \delta U + f\delta x\right] dt = 0 \tag{1}$$

where T, U and $f\delta x$ terms are defined by:

$$U = \frac{1}{2}\int_{V_S} \underline{S}^T \underline{T}\, dV_s + \frac{1}{2}\int_{V_P} \underline{S}^T \underline{T}\, dV_p - \int_{V_P} \underline{E}^T \underline{D}\, dV_p \tag{2}$$

$$T = \frac{1}{2}\int_{V_S} \rho_s \underline{\dot{u}}^T \underline{\dot{u}}\, dV_s + \frac{1}{2}\int_{V_P} \rho_s \underline{\dot{u}}^T \underline{\dot{u}}\, dV_p \tag{3}$$

$$f\delta x = \sum_{i=1}^{nf} \delta \underline{u}(x_i) \cdot \underline{f_i}(x_i) - \sum_{j=1}^{nq} \delta \underline{v} \cdot \underline{q_j} \tag{4}$$

where U is the potential energy, T is the kinetic energy, $f\delta x$ is the external work applied to the system, S is the strain, T is the stress, E is the electric filed, D is the electric displacement, V is the volume, u is the displacement, x is the position along the beam, v is the applied voltage, q is the

charge, ρ is the density *f* is the applied force and the subscripts *p* and *s*, represent the piezoelectric material and the substrate, respectively. Before the variational indicator can be used to solve for the equations of motion the piezoelectric constitutive equations need to be introduced into the potential energy term and the variation of both the potential and kinetic energy must be found. First the piezoelectric constitutive equations will be introduced, which are:

$$\begin{bmatrix} \underline{T} \\ \underline{D} \end{bmatrix} = \begin{bmatrix} c^E & -e^T \\ e & \varepsilon^S \end{bmatrix} \begin{bmatrix} \underline{S} \\ \underline{E} \end{bmatrix} \tag{5}$$

where *c* is the modulus of elasticity, ε is the dielectric constant and the superscript, $(\,)^S$, signifies the parameter was measured at constant strain and the superscript, $(\,)^E$, indicates the parameter was measured at constant electric field (short circuit). These constitutive equations relate the electrical and mechanical properties of the piezoelectric element. The specification of these relationships will allow electromechanical interaction to be included in the model. The term *e* is the piezoelectric coupling coefficient and relates the stress to the applied electric field. The piezoelectric coupling coefficient can be written as shown in equation 6 in terms of the more commonly specified coupling coefficient *d* by:

$$e = d_{ij} c^E \tag{6}$$

where *c* is the d_{ij} is the piezoelectric coupling coefficient with the subscript *i* and *j* referring to the direction of the applied field and the poling, respectively. Now we can incorporate the piezoelectric properties in the potential energy function:

$$\begin{aligned} U = \frac{1}{2}\Big[& \int_{V_S} \underline{S}^T c_s \underline{S}\, dV_S + \int_{V_P} \underline{S}^T c^E \underline{S}\, dV_p \\ & - \int_{V_P} \underline{S}^T e^T \underline{E}\, dV_P - \int_{V_P} \underline{E}^T e \underline{S}\, dV_P \\ & - \int_{V_P} \underline{E}^T \varepsilon^S \underline{E}\, dV_P \Big] \end{aligned} \tag{7}$$

Taking the variation of the kinetic energy from equation 3, and the potential energy term containing the piezoelectric properties of equation 7, yields:

$$\begin{aligned}\delta U = &\int_{V_S} \delta \underline{S}^T c_s \underline{S}\, dV_S + \int_{V_P} \delta \underline{S}^T c^E \underline{S}\, dV_p \\ &- \int_{V_P} \delta \underline{S}^T e^T \underline{E}\, dV_P - \int_{V_P} \delta \underline{E}^T e \underline{S}\, dV_P \\ &- \int_{V_P} \delta \underline{E}^T \varepsilon^S \underline{E}\, dV_P\end{aligned} \tag{8}$$

$$\delta T = \int_{V_S} \rho_s \delta \dot{\underline{u}}^T \dot{\underline{u}}\, dV_s + \int_{V_P} \rho_p \delta \dot{\underline{u}}^T \dot{\underline{u}}\, dV_p \tag{9}$$

The variations found in equations 4, 8 and 9 can be substituted into equation 1 to obtain the variational indicator:

$$\begin{aligned}V.I. = \int_{t_1}^{t_2} \Bigg[&\int_{V_S} \rho_s \delta \dot{\underline{u}}^T \dot{\underline{u}}\, dV_s + \int_{V_P} \rho_p \delta \dot{\underline{u}}^T \dot{\underline{u}}\, dV_p \\ &- \int_{V_S} \delta \underline{S}^T c_s \underline{S}\, dV_S - \int_{V_P} \delta \underline{S}^T c^E \underline{S}\, dV_p \\ &+ \int_{V_P} \delta \underline{S}^T e^T \underline{E}\, dV_P + \int_{V_P} \delta \underline{E}^T e \underline{S}\, dV_P \\ &+ \int_{V_P} \delta \underline{E}^T \varepsilon^S \underline{E}\, dV_P + \sum_{i=1}^{nf} \delta \underline{u}(x_i) \cdot \underline{f}(x_i) - \sum_{j=1}^{nq} \delta \underline{v} \cdot \underline{q_j} \Bigg]\end{aligned} \tag{10}$$

This equation can now be used to solve for the equations of motion of any mechanical system containing piezoelectric elements. In order to solve equation 10 for the cantilever beam with bimorph piezoelectric elements some assumptions must be made. The first assumption follows the Rayleigh-Ritz procedure, which says that the displacement of the beam can be written as the summation of modes in the beam and a temporal coordinate (Inman, 2001):

$$u(x,t) = \sum_{i=1}^{N} \phi_i(x) r_i(t) = \underline{\phi}(x) \underline{r}(t) \tag{11}$$

where $\Phi_i(x)$ is the assumed mode shapes of the structure which can be set to satisfy any combination of boundary conditions, $r(t)$ is the temporal coordinate of the displacement and N is the number of modes to be included in the analysis. The second assumption made is to apply the Euler-Bernoulli beam theory. This allows the stain in the beam to be written as the product of the distance from the neutral axis and the second derivative of displacement with respect to the

position along the beam. Once the strain is defined in this way equation 11 can be used define the strain as follows:

$$\underline{S} = -y\frac{\partial^2 u(u,t)}{\partial x^2} = -y\phi(x)'' r(t) \tag{12}$$

The third and last assumption is that the electric potential across the piezoelectric element is constant. This assumption also indicates that no field is applied to the beam, which in latter equations designates the beam to be inactive material:

$$\underline{E} = \psi(y)v(t) = \begin{cases} -v/t_p & t/2 < y < t/2 + t_p \\ 0 & -t/2 < y < t/2 \\ v/t_p & -t/2 - t_p < y < -t/2 \end{cases} \tag{13}$$

The previous assumption is for a beam with bimorph piezoelectric elements on the top and bottom of the beam as shown in Figure 1. The beam in Figure 1 also shows the notation for the geometry of the beam that is used throughout the derivation.

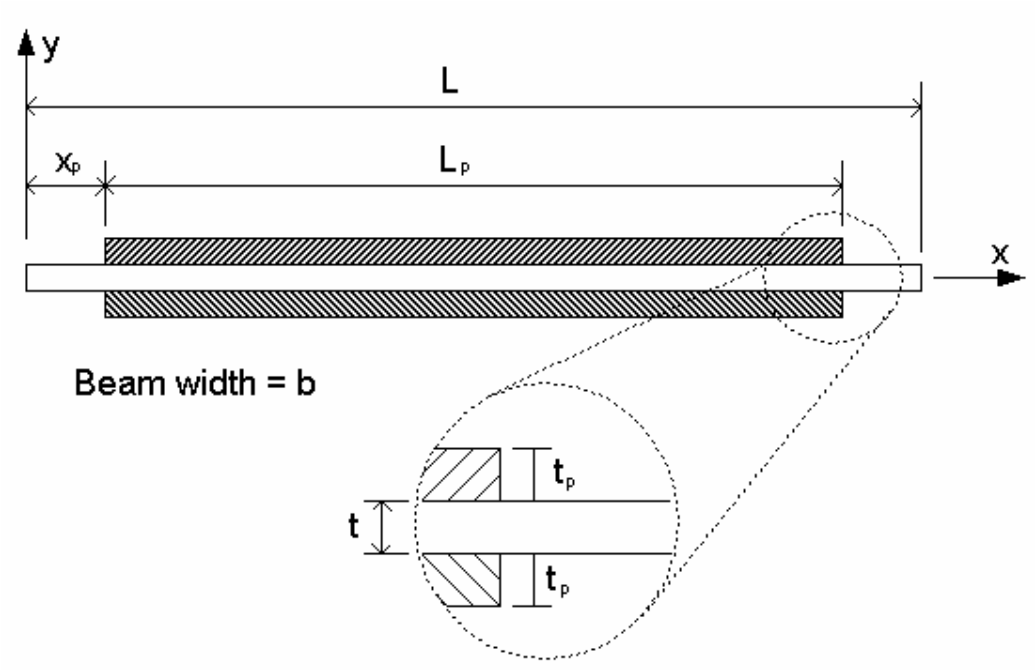

Figure 1: Schematic of beam describing the variables.

Using the previous assumptions we can simplify the variational indicator to include terms that represent physical parameters. By doing this the equations describing the system become more recognizable when compared to those of a typical system and help give physical meaning to the parameters in the equations of motion. The mass matrices for the system can be written as:

$$M_s = \int_{V_S} \rho_s \underline{\phi}^T(x)\underline{\phi}(x)dV_s$$

$$M_p = \int_{V_P} \rho_p \underline{\phi}^T(x)\underline{\phi}(x)dV_p \tag{14}$$

The stiffness matrices can be written as:

$$K_s = \int_{V_S} y^2 \underline{\phi}^T(x)'' c_s \underline{\phi}(x)'' dV_s$$

$$K_p = \int_{V_P} y^2 \underline{\phi}^T(x)'' c^E \underline{\phi}(x)'' dV_p \tag{15}$$

The electromechanical coupling matrix, Θ, and the capacitance matrix, C_p, are defined by:

$$\Theta = -\int_{V_P} y\underline{\phi}^T(x)'' e^T \psi(y)dV_p$$

$$C_p = \int_{V_p} \psi^T(y)\varepsilon^S\psi(y)dV_p \tag{16}$$

The parameters defined in equations 14, 15 and 16 can be substituted into variational indicator of equation 10. This substitution allows the variational indicator to be written as:

$$\begin{aligned} \text{V.I.} = \int_{t_1}^{t_2} \Big[& \delta\dot{\underline{r}}^T(t)(M_s + M_p)\dot{\underline{r}}(t) - \delta\underline{r}^T(t)(K_s + K_p)\underline{r}(t) \\ & + \delta\underline{r}^T(t)\Theta v(t) + \delta v(t)\Theta^T\underline{r}(t) + \delta v(t)C_p v(t) \\ & + \sum_{i=1}^{nf} \delta\underline{r}(t)\phi(x_i)^T f_i(t) - \sum_{j=1}^{nq} \delta\underline{v}q_j(t) \Big] dt = 0 \end{aligned} \tag{17}$$

where δ() indicates the variation of the corresponding variable. Taking the integral of the variational indicator leaves two coupled equations. The two equations shown below are coupled by the previously defined electromechanical coupling matrix Θ. The top equation defines the mechanical motion and the bottom equation defines the electrical properties of the system:

$$\begin{aligned}\left(M_s + M_p\right)\underline{\ddot{r}}(t) + \left(K_s + K_p\right)\underline{r}(t) - \Theta v(t) &= \sum_{i=1}^{nf} \phi(x_i)^T f_i(t) \\ \Theta^T r(t) + C_p v(t) &= q(t)\end{aligned} \tag{18}$$

These equations now represents the electro-mechanical system and can be used to determine the motion of the beam, however this system of equations does not contain any energy dissipation. Because the model is intended to represent a power harvesting system that must be removing energy, this form is not suitable for our needs, as it does not account for energy lost through the structure. In addition, the energy removed from the system through energy harvesting must be accounted for. To incorporate energy dissipation into the equation one can use ohm's law and add a resistive element between the positive and negative electrodes of the piezoelectric. The resistive element will provide a means of removing energy from the system. Then electrical boundary condition becomes:

$$v_i(t) = -R\dot{q}(t) \tag{19}$$

In addition, the system should have some type of additional mechanical damping that needs to be accounted for. If only the electrical damping is accounted for, the model will over predict the actual amount of power generated. The amount of mechanical damping added to the model was determined from experimental results. This is done using proportional damping methods and the damping ratio that is predicted from the measured frequency response function. With the damping ratio known, proportional damping can be found from (Inman, 2001):

$$C = \alpha\left(M_s + M_p\right) + \beta\left(K_s + K_p\right) \tag{20}$$

where α and β are determined from:

$$\zeta_i = \frac{\alpha}{2\omega_i} + \frac{\beta\omega_i}{2} \quad i = 1,2,...n \tag{21}$$

where ζ_i is the damping ratio found from the frequency response of the structure. Incorporating equations 19 and 20 into equation 18, results in the final model of the power harvesting system:

$$\begin{gathered}\left(M_s + M_p\right)\underline{\ddot{r}}(t) + C\underline{\dot{r}}(t) + \left(K_s + K_p\right)\underline{r}(t) - \Theta v(t) = \sum_{i=1}^{nf} \phi(x_i)^T f_i(t) \\ R\dot{q}(t) - C_p^{-1}\Theta^T r(t) + C_p^{-1} q(t) = 0\end{gathered} \tag{22}$$

Equation 22 shown above provides an accurate model of the power harvesting system. The $\dot{q}(t)$ term provides the current output of the piezoelectric element and can be directly related to the power output of the piezoelectric through the load resistance *R*.

The last portion of our model left undefined is the forcing function. The system that will be investigated is a cantilever beam that is excited by transverse vibrations of the structure that it is clamped to; therefore no force is directly applied to the beam. Instead the clamped end of the beam is experiencing base motion and transferring that energy to the beam through its own inertia. The standard boundary conditions of the clamped end of the beam say that the slope and displacement are zero at all time. For the condition of base motion the zero displacement condition would not be held and a new set of mode shapes would need to be generated. Rather than doing this, it was decided that a force corresponding to the inertia of the beam when subjected to the base motion could be used and the clamped-free mode shapes would still be valid. The forcing function used to model the inertia of the beam is:

$$f(t) = \int_0^L \int_0^b \int_0^t \rho A \omega^2 \sin(\omega t) dz dy dx \tag{23}$$

With the forcing function defined everything necessary to simulate the power harvesting system is included in the model. The following sections of this paper will describe the experimental procedures and results, in order to demonstrate the accuracy of this model.

Experimental Setup for Model Verification

The accuracy of the model will be tested on a Midé Technology Corporation Quick Pack model QP40N, although it could be used to model any beam with a piezoelectric attached. The QP40N is a bimorph actuator with dimensions and properties shown in Figure 2. The Quick Pack actuator is constructed from four piezoceramic wafers embedding in a Kapton and epoxy matrix. Experiments were performed to verify the accuracy of the models ability to predict the amount of power generated from this device when subjected to transverse vibrations of varying frequency and amplitude. As mentioned previously we were interested in the Quick Pack being mounted with cantilever boundary conditions. To provide the transverse vibration, the Quick Pack was mounted actuator to an electromagnetic shaker as shown in Figure 3.

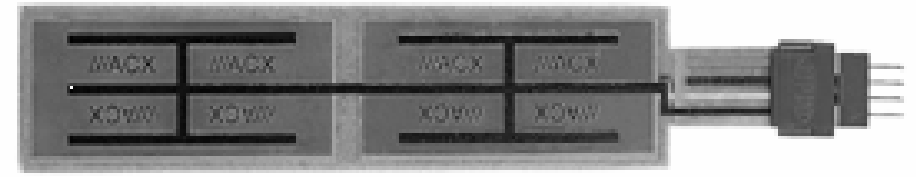

Device size (mm): 100.6 x 25.4 x 0.762
Device weight (g): 9.52
Active elements: 2 stacks of 2 piezos
Piezo wafer size (mm): 45.974 x 20.574 x 0.254
Full scale voltage range (V): ±200

Figure 2: Midé Technology Corporation Quick Pack model QP40N (from Midé Technology Corporation).

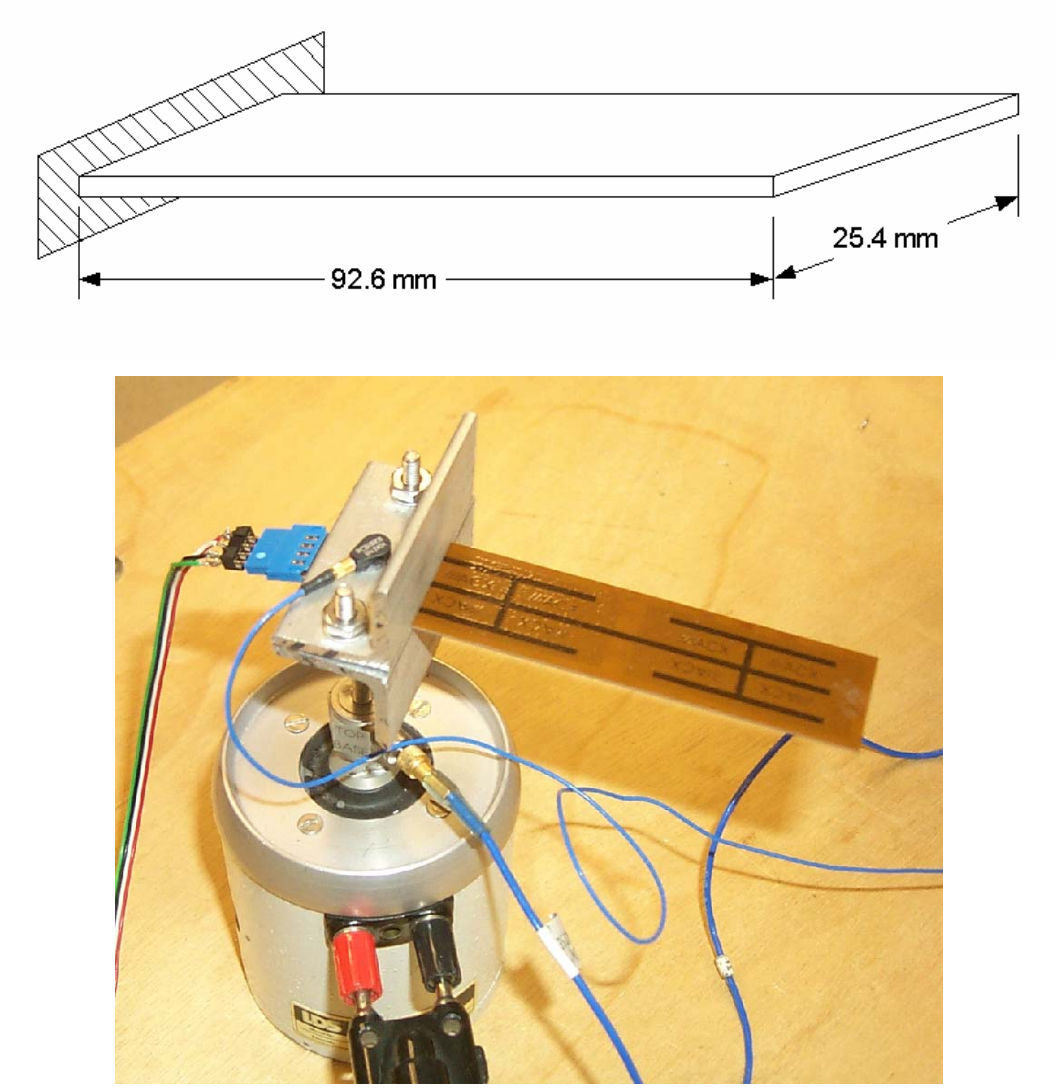

Figure 3: Quick Pack QP40N attached to the shaker and dimensions of beam when one end is clamped.

One complication that arose when modeling the Quick Pack actuator was due to its composite structure and the piezoelectric wafers not spanning the entire length of the beam, which can be seen in Figure 2. Because the area of the beam with no piezoelectric wafer consisted of only Kapton and epoxy, it contained a localized area with a lower modulus of elasticity. Midé Technology Corporation could not specify a value for the effective modulus of the complete beam. Therefore, the setup shown in Figure 4 was constructed to measure the stiffness of the Quick Pack. To obtain a value for the stiffness the force applied to the beam and its corresponding deflection needed to be measured. The experimental setup consists of a

Transducer Techniques 100 gram load cell model GSO-100C and a Polytec laser vibrometer. The load cell was mounted on a lead screw to allow a steady force to be applied at the tip of the beam. The results of this test found the modulus of the beam to be 2.5 GPa. The reason for this value being so low is due to the area at the mid-span of the beam that consisted of only the Kapton and epoxy. When the static tests were performed on the beam it was apparent that the majority of the bending was occurring at this location. Therefore, it was concluded that the experimental tests performed had actually measured the modulus of elasticity corresponding to the Kapton and epoxy portion of the beam. This still left the overall modulus of the beam unknown. The value calculated for the overall the modulus of the beam was found by simply averaging the modulus of the piezoelectric material, that was supplied by Midé and the experimentally found modulus for the Kapton and epoxy matrix according to their individual percent of the cross sectional area. The resulting modulus of elasticity and the other piezoelectric properties used are shown in Table 1.

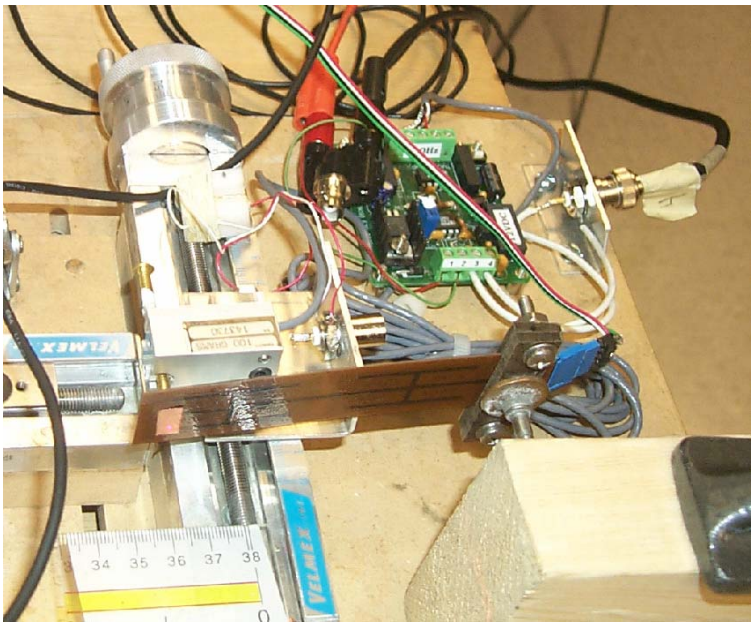

Figure 4: Experimental setup used to find the elastic modulus of the Kapton-epoxy matrix.

Table 1: Properties of the Quick Pack

Property	Symbol	Value
Dielectric Constant	k_3^T	1800
Piezoelectric Strain Coefficient	d_{13}	-179x10^{-12} m/volt
Modulus of Piezoelectric	c^E	63 GPa
Modulus of Kapton-epoxy	c_s	2.5 Gpa
Modulus of Quick Pack	c_b	35.17 GPa
Density of Piezo Material	ρ	7700 kg/m^3
Density Composite Matrix	ρ	2150 kg/m^3

Model Verification

The accuracy of the model was compared against experimental results to demonstrate the ability of the model to accurately predict the amount of power produced by the Quick Pack when subjected to transverse vibration. To ensure that the model and experimental tests were subjected to the same excitation force an accelerometer was used to calculate the amplitude of the sinusoidal force applied to the beam through:

$$a = A\omega^2 \sin(\omega t) \Rightarrow A_{\max} = \frac{a}{\omega^2} \tag{24}$$

where a is the acceleration of the clamped end of the beam. The beam was excited by a sinusoidal input and the steady state power output was measured across several different resistors. The frequency response of the model and the experimentally tested Quick Pack are shown in Figure 5. The differences in the two responses are attributed to the Quick Pack's composite structure resulting in coupled modes and the nonlinear properties of the Kapton material, especially its modulus of elasticity that varies nonlinearly with frequency. Additionally, looking at the mode shapes of a cantilever beam shown in Figure 6 it can be seen that in the second mode a large amount of bending occurs at the beam's midsection. However the Quick Pack has an area of low stiffness at the midsection but due to the use of a uniform modulus of elasticity and density in the model, the stiffness is increased at this location and the predicted frequency of the second

mode is higher than measured. It is expected that a beam constructed of a homogeneous material with a piezoelectric mounted to is surface would produce a more accurate frequency response.

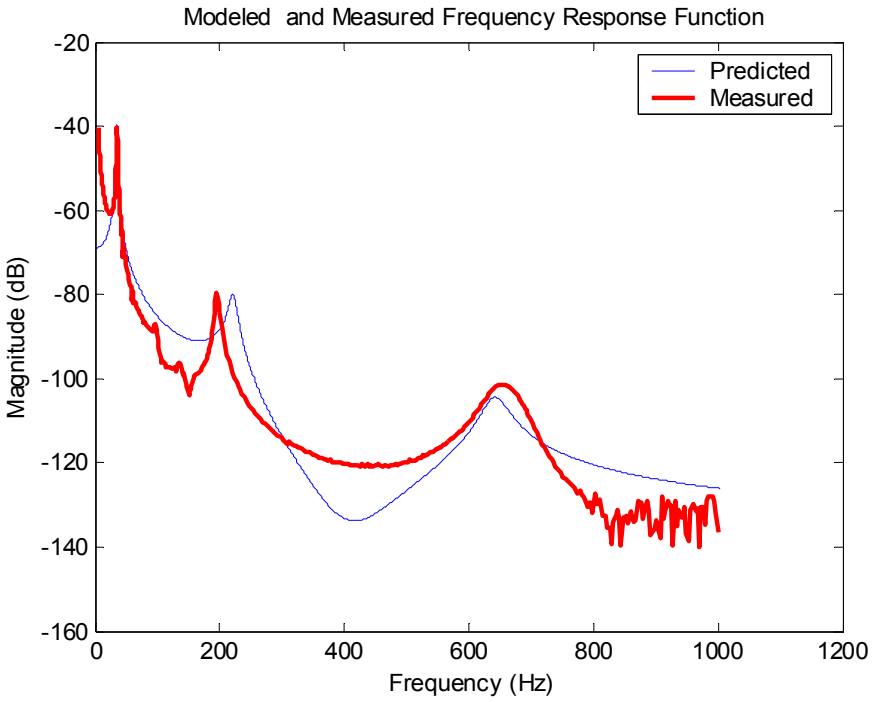

Figure 5: Frequency response of the model and the experimental data.

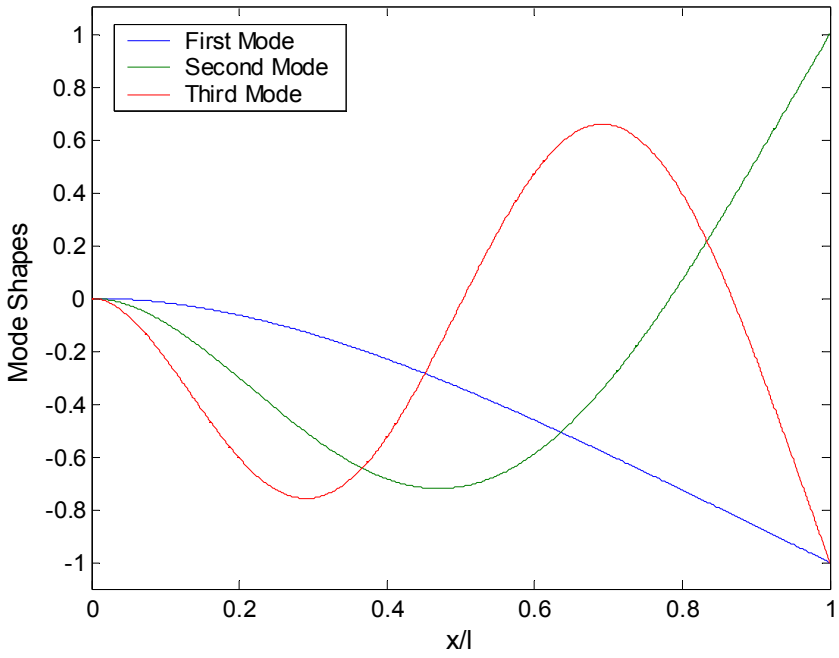

Figure 6: First three mode shapes of a cantilever beam.

The measured current generated by the Quick Pack was compared to the predicted current from the model for various frequencies and load resistances. The output current across a 10kΩ resistor for several excitation frequencies of the model and the measured current obtained through experiments are shown in Figures 6, 7 and 8. Figures 9 and 10 show the output current across a 100Ω load resistance at 25Hz and 50Hz, respectively, and Figures 11 and 12 show the output current across a 100kΩ load resistor at 25Hz and 50Hz, respectively. The predicted response shown in these Figures shows a transient response for a small period of time while the experimental results do not because they were recorded at steady state vibration. Table 2 provides an approximate list of the measured and predicted currents generated for numerous values of frequency and load resistance. The values in this table demonstrate that the model provides a very accurate measurement of the power generated at various frequencies and resistive loads. This shows that the model would be effective as a design tool for determining the ideal size and excitation level necessary to provide the desired power.

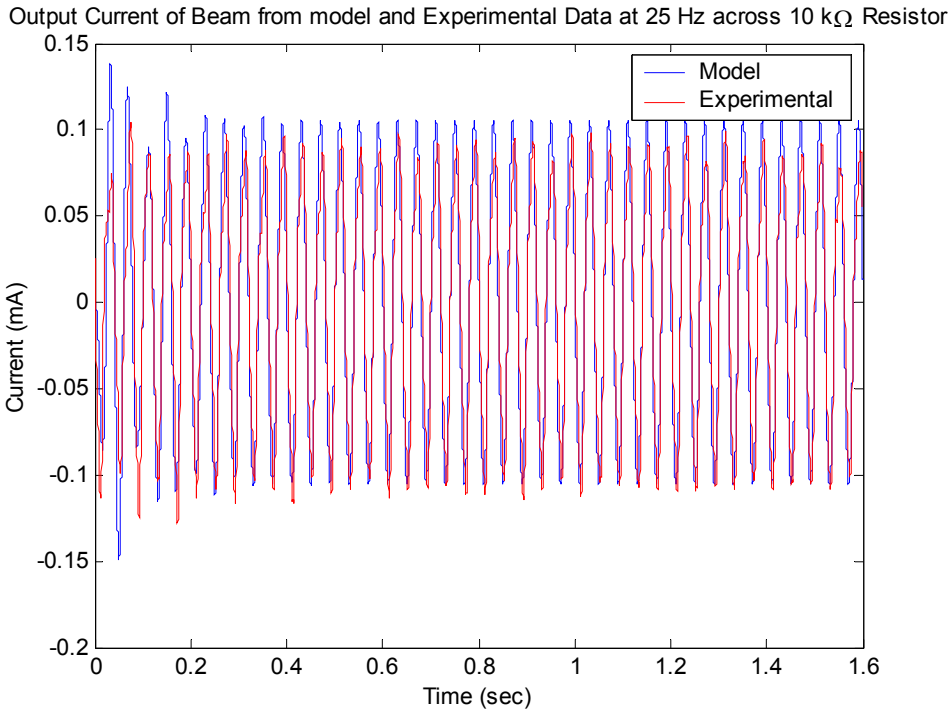

Figure 6: Output current predicted by model and measured across a 10KΩ resistor at 25Hz.

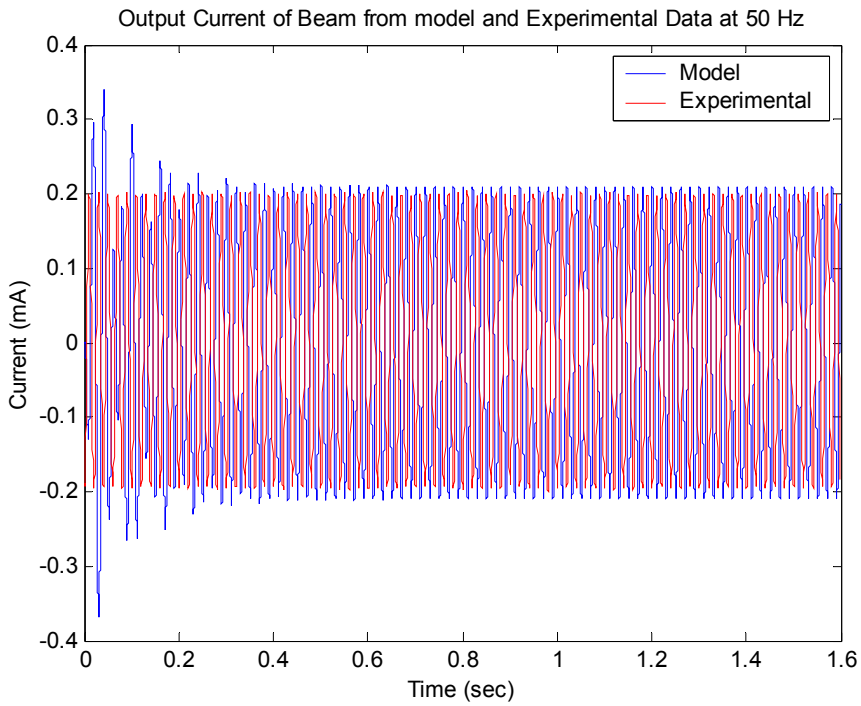

Figure 7: Output current predicted by model and measured across a 10KΩ resistor at 50Hz.

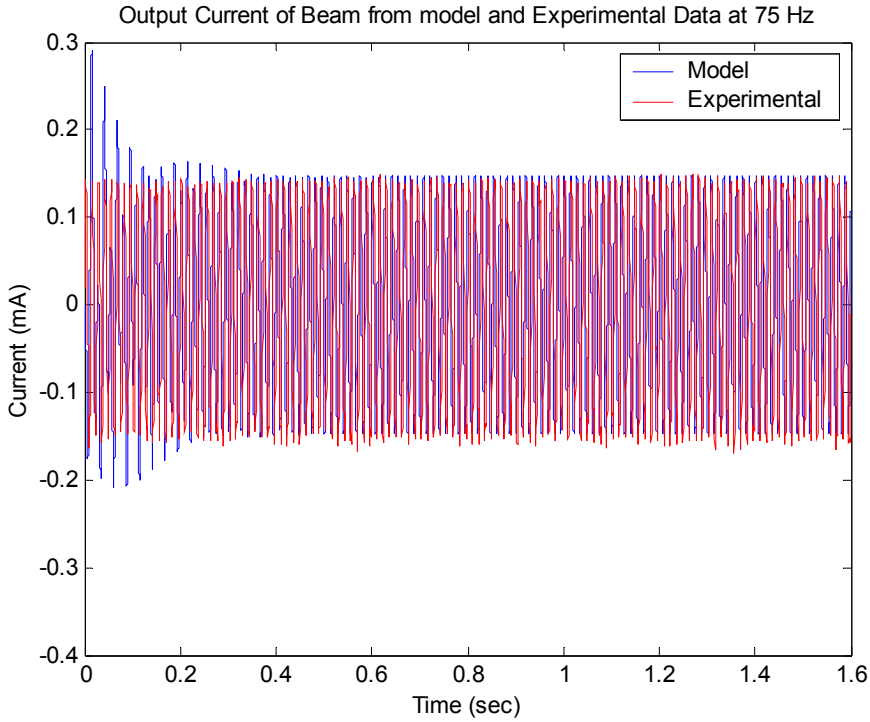

Figure 8: Output current predicted by model and measured across a 10KΩ resistor at 75Hz.

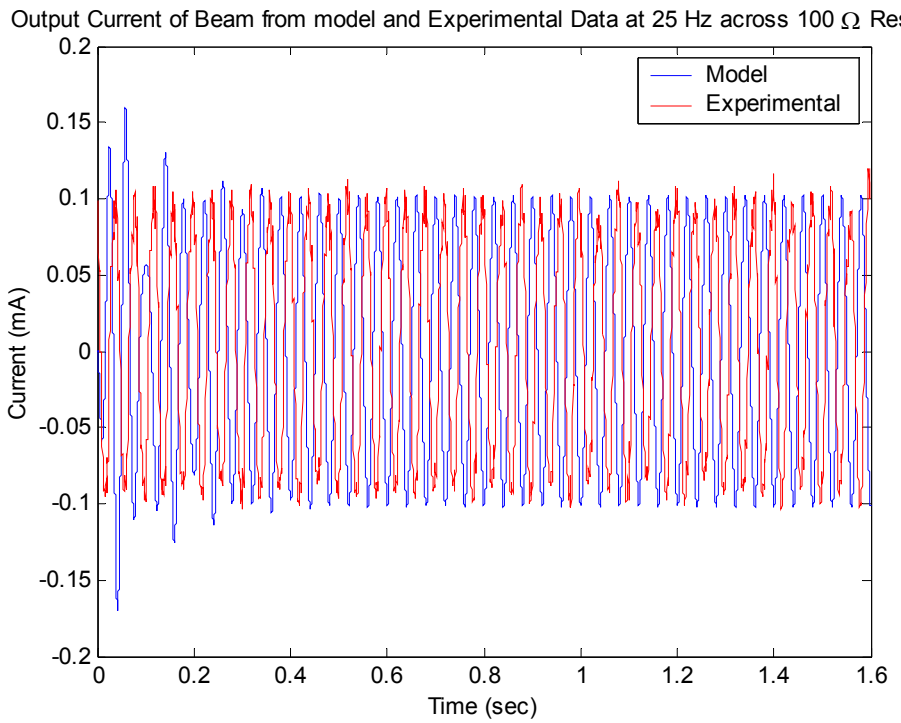

Figure 9: Output current predicted by model and measured across a 100Ω resistor at 25Hz.

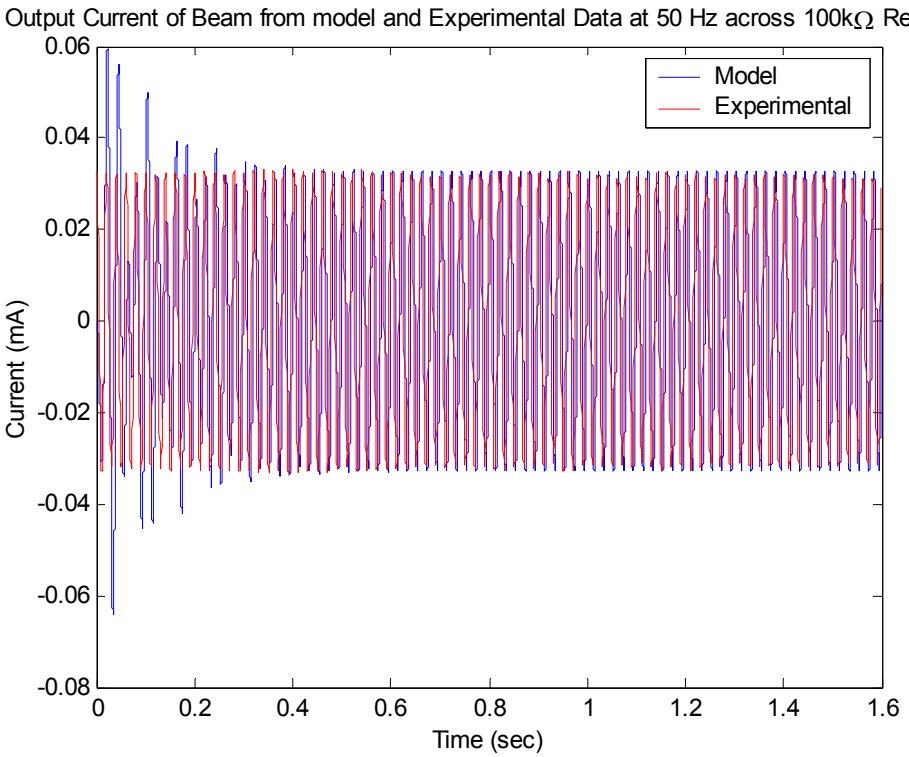

Figure 10: Output current predicted by model and measured across a 100KΩ resistor at 50Hz.

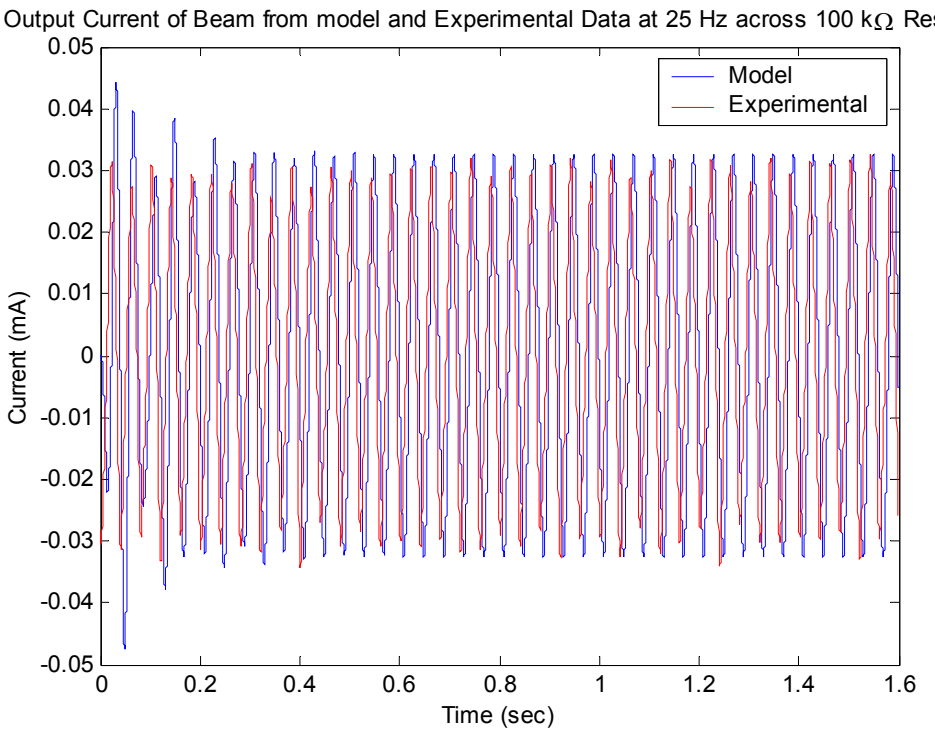

Figure 11: Output current predicted by model and measured across a 10KΩ resistor at 50Hz.

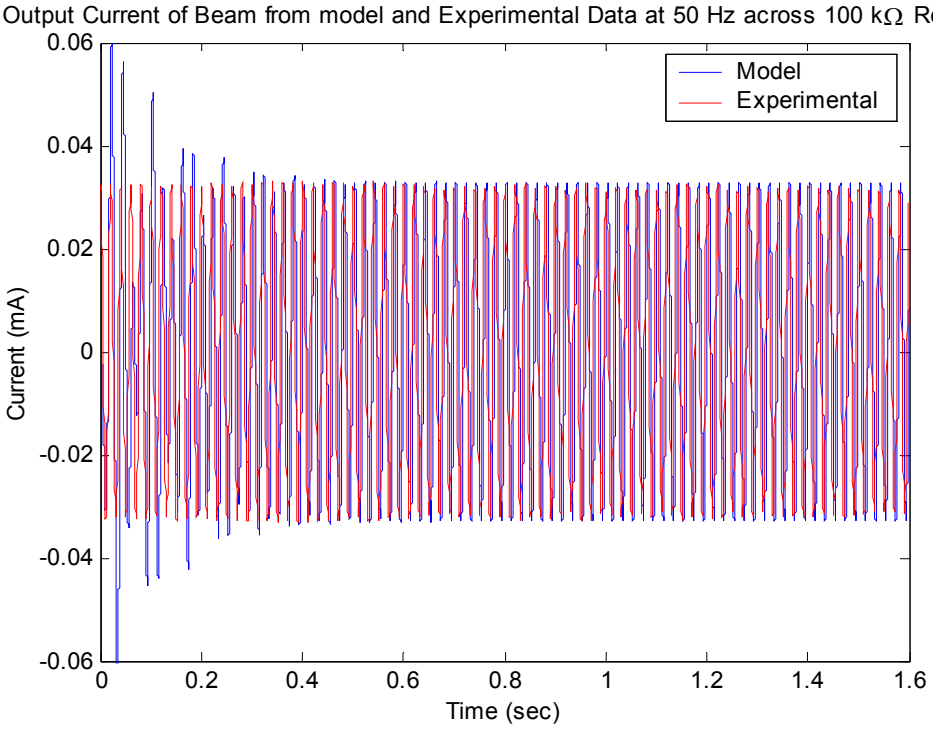

Figure 12: Output current predicted by model and measured across a 100KΩ resistor at 50Hz.

Table 2: Amplitude of measured and simulated current.

Frequency	Load Resistance	Simulated Current	Measured Current	Percent Error
25 Hz	100 Ω	0.101mA	0.104mA	2.97%
25 Hz	10 kΩ	0.105mA	0.106mA	0.95%
25 Hz	100 kΩ	0.032mA	0.032mA	0.00%
30 Hz	100 Ω	0.360mA	0.345mA	4.17%
30 Hz	10 kΩ	0.295mA	0.30mA	1.67%
30 Hz	100 kΩ	0.065mA	0.068mA	4.61%
50 Hz	100 Ω	0.20mA	0.20mA	0.00%
50 Hz	10 kΩ	.175mA	.180mA	2.86%
50 Hz	100 kΩ	0.033mA	0.032mA	3.03%
75 Hz	10 kΩ	0.142mA	0.144mA	1.41%
150 Hz	10 kΩ	0.0132mA	0.0133mA	0.75%

Disscusion of Power Harvesting and Shunt Damping

In addition to providing an accurate estimate of the of the power generated by a beam with a complicated piezoelectric layout and a non-homogeneous material composition, the model also demonstrates that power harvesting works much like a shunt damper. When a power harvesting system is implemented, energy is removed from the system and supplied to the desired electrical components. Due to the removal of energy from the system conservation of energy says that increased damping must occur. This is the same principle that is used in shunt damping systems. However, when implementing shunt circuits it is often advantageous to use a RLC circuit that allows the circuit to be tuned to the resonant frequency of the system for maximum power dissipation. In the case of the power harvesting system that has been investigated in this paper a constant load resistance was used which will also induce damping into the system but over a broad range of frequencies rather than the turned frequency of a RLC circuit. The damping effect caused by power harvesting on the impulse response of a beam for three different load resistances is shown in Figures 13, 14 and 15. In Figure 13 the load resistance is set at a low value of 100Ω, which does not dissipate a large amount of energy causing only a small amount of damping to be added to the system. In the case of Figure 14 the load resistance is set at an ideal value of 10kΩ allowing the maximum flow of energy from the piezoelectric device and in turn

causing higher damping that is apparent in the increased settling time of the response. Now looking at Figure 15, the load resistance is further increased to 100kΩ giving the system the ability to dissipate a large amount of energy from the system. However, when the load resistance becomes very high the ability of energy to flow from the piezoelectric material is reduced causing the damping induced in the system to decrease. These Figures demonstrate the effect of power harvesting on the dynamics of a structure. It is apparent that as more energy is removed from the system the impulse dies out faster until a critical level is reached, after which the resistive load of the circuit exceeds the impedance of the piezoelectric network causing lower efficiency power generation and for this example lower energy dissipation to the beam. This study shows that the effects of power harvesting on the dynamics of a mechanical system are very similar to those of shunt damping, with the major difference being that the energy is stored for use rather than of dissipated.

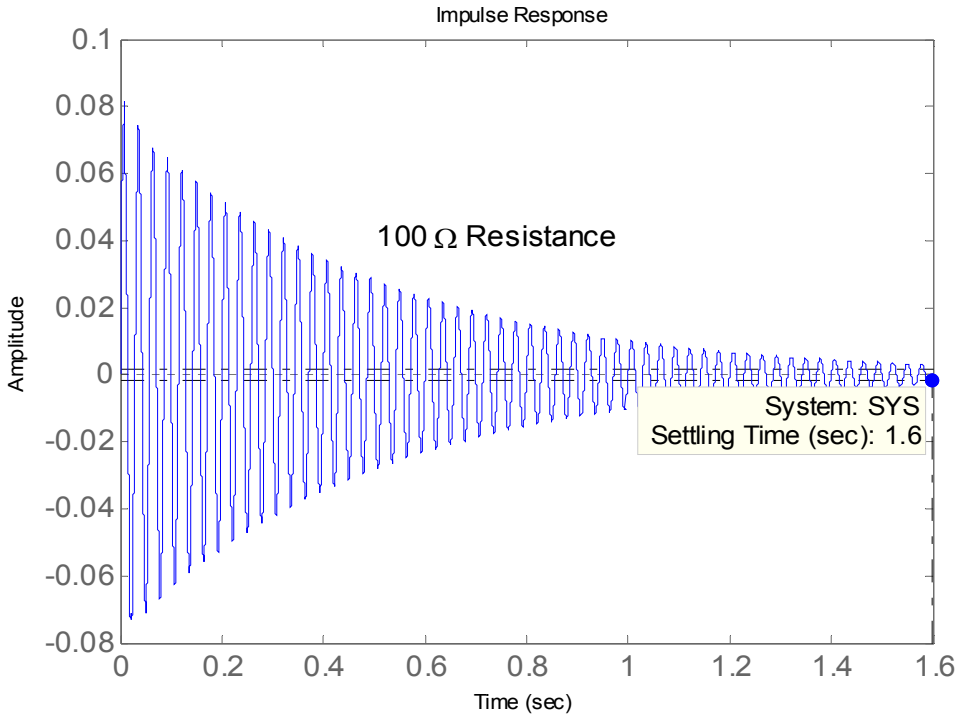

Figure 13: Impulse response with a 100Ω resistive load.

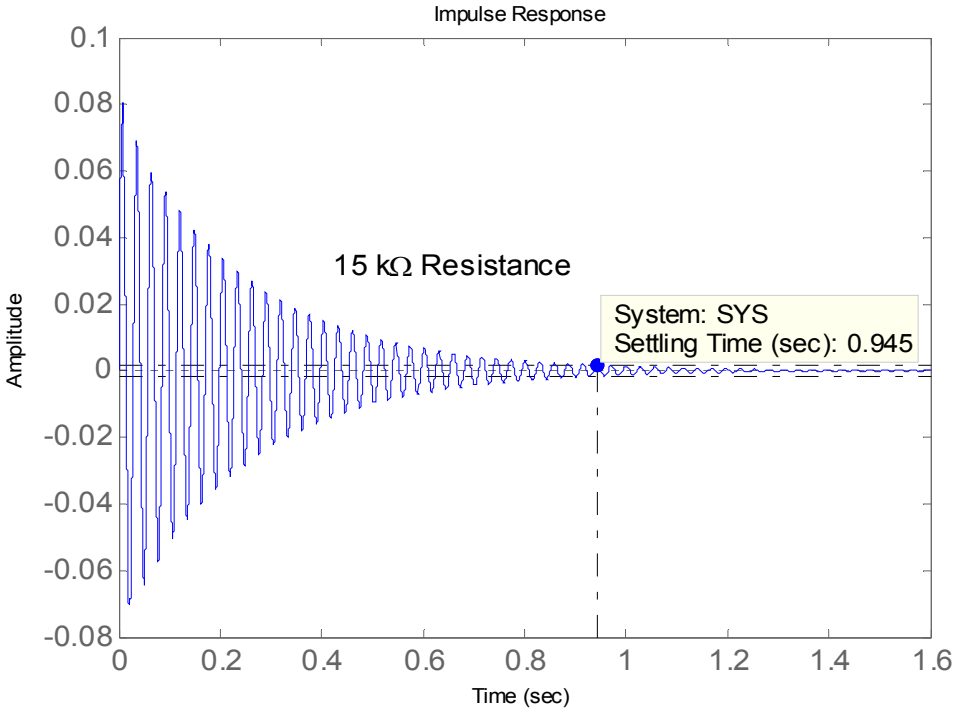

Figure 14: Impulse response with a 15kΩ resistive load.

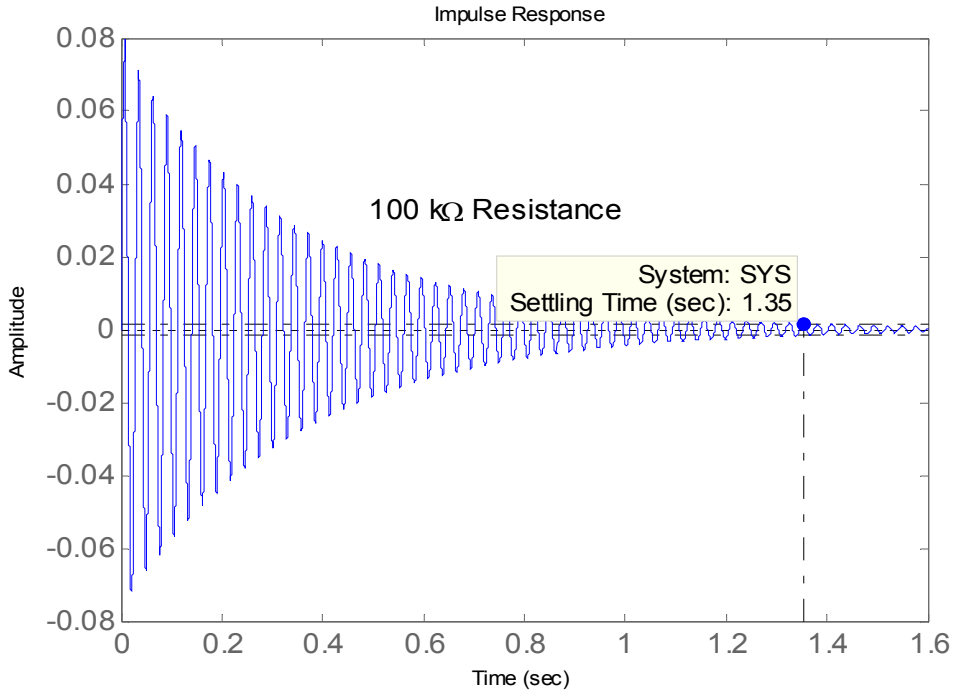

Figure 15: Impulse response with a 100kΩ resistive load.

Conclusions

One method of performing power harvesting is to use piezoelectric materials that can convert the ambient vibration energy surrounding them into electrical energy. This electrical energy can then be used to power other devices or stored for later use. This technology has gained an increasing large amount of attention due to the recent advances in wireless and MEMS technology allowing sensors to be placed in remote locations and operate at very low power. The need for power harvesting devices is caused by the use batteries as power supplies for these wireless electronics. Since the battery has a finite lifespan, once extinguished of its energy, the sensor must be recovered and the battery replaced for the continued operation of the sensor. This practice of obtaining sensors solely to replace the battery can become and expensive task, because their wireless nature allows them to be placed in exotic locations. Therefore, methods of harvesting the energy around these sensors must be implemented to expand the life of the battery or ideally provide an endless supply of energy to the sensor for its lifetime.

This Paper has developed a model to predict the amount of power capable of being generated through the vibration of a cantilever beam with attached piezoelectric elements. The derivation of the model has been provided, allowing it to be applied to a beam with various boundary conditions or layout of piezoelectric patches. The model was verified using experimental results and proved to be very accurate independent of excitation frequency and load resistance. In addition, the verification of the model was performed on a structure the contained a complex piezoelectric layout and a non-homogenous material beam, indicating that the model is robust and can be applied to a variety of different mechanical conditions. The damping effects of power harvesting were also shown to be predicted in the model and to follow that of a resistive shunt damping circuit. This model provides a design tool for developing power harvesting systems by assisting in determining the size and extent of vibration needed to produce the desired level of power generation. The potential benefits of power harvesting and the advances in low power electronics and wireless sensors are making the future of this technology look very bright.

References

Face International Corporation, http://www.face-int.com.

Clark, W. and Ramsay, M. J., 2001. "Smart Material Transducers as Power Sources for MEMS Devices," Proceedings of SPIE's 8th Annual International Symposium on Smart Structures and Materials, San Diego, California, USA, Vol. 4332 2001, pp. 429-438..

Crawley, E.F., Anderson, E.H., 1990, "Detailed Models of Piezoceramic Actuation of Beams," *Journal of Intelligent Material Systems and Structures*, Vol. 1, no. 1, p. 4-25.

Elvin, N.G. and Elvin, A.A., and Spector, M., 2001, "A Self-Powered Mechanical Strain Energy Sensor," *Smart Materials and Structures*, Vol. 10, pp. 293-299.

Elvin, N.G., Elvin, A.A., and Spector, M., 2000, "Implantable bone strain telemetry system and method," US Patent Specification 6034296.

Goldfarb, M. and Jones, L.D., 1999, "On the Efficiency of Electric Power Generation with Piezoelectric Ceramic," *ASME Journal of Dynamic Systems, Measurement, and Control*, Vol. 121, September, pp. 566-571.

Hagwood, N.W., Chung, W.H., Von Flowtow, A., 1990, "Modelling of piezoelectric Actuator Dynamics for Active Structural Control," *Journal of Intelligent Material Systems and Structures*, Vol. 1, no. 3, p. 327-354.

Inman, D.J., 2001, Engineering Vibration," Prentice-Hall, Inc., Upper Saddle River, New Jersey.

Kasyap, A., Lim, J., Johnson, D., Horowitz, S., Nishida, T., Ngo, K., Sheplak, M. and Cattafesta, L., 2002, "Energy Reclamation from a Vibrating Piezoceramic Composite Beam," Proceedings of 9th International Congress on Sound and Vibration, Orlando, FL, Paper No. 271.

Kimura, M, 1998,"Piezoelectric Generation Device", US Patent Number 5,801,475.

Kymissis, J., Kendall, C., Paradiso, J. and Gershenfeld, N., 1998, "Parasitic Power Harvesting in Shoes," Second IEEE International Symposium on wearable Computers, October 19-20th, Pittsburg, PA, pp. 132-139.

Ottman, G.K., Hofmann, H., Bhatt A. C. and Lesieutre, G. A., 2002, "Adaptive Piezoelectric Energy Harvesting Circuit for Wireless, Remote Power Supply," *IEEE Transactions on Power Electronics*, Vol. 17, No.5, pp. 669-676.

Smits, J., Dalke, S., Cooney, T.K., 1991, "The Constituent Equations of Piezoelectric Bimorphs," *Sensors and Actuators*, Vol. 28, pp. 41-61.

Sodano, H.A., Magliula, E.A., Park, G. and Inman, D.J., 2002, "Electric Power Generation from Piezoelectric Materials," The 13th International Conference on Adaptive Structures and Technologies, October 7-9th, Potsdam/Berlin, Germany.

Sodano, H.A., Park, G., Leo, D.J. and Inman, D.J., 2003, "Use of Piezoelectric Energy Harvesting Devices for Charging Batteries," SPIE's 10th Annual International Symposium on Smart Structures and Materials, March 2-6th, San Diego, CA, On CD.

Starner, T., 1996, "Human-Powered Wearable Computing," *IBM Systems Journal*, Vol. 35 No.3-4, pp. 618-628.

Umeda, M., Nakamura, K. and Ueha, S., 1996, "Analysis of Transformation of Mechanical Impact Energy to Electrical Energy Using a Piezoelectric Vibrator," *Japanese Journal of Applied Physics*, Vol. 35, Part1, No. 5B, May, pp. 3267-3273.

Umeda, M., Nakamura, K. and Ueha, S., 1997, "Energy Storage Characteristics of a Piezo-Generator using Impact Induced Vibration," *Japanese Journal of Applied Physics*, Vol. 36, Part 1, No. 5B, May, pp. 3146-3151.